Colloidal Gas Aphrons (CGA): Dispersion and Structural Features

Paula Jauregi
Kluyver Institute for Biotechnology, Delft University of Technology, 2628 BC Delft, The Netherlands

Geoffrey R. Mitchell
Dept. of Physics, The University of Reading, Reading RG6 6AP, England

Julie Varley
Dept. of Chemical Engineering and Chemical Technology, Imperial College, London SW7 2B7, England

Colloidal gas aphrons (CGA) have previously been defined as surfactant stabilized gas microbubbles and characterized for a number of surfactants in terms of stability, gas holdup and bubble size even though there is no conclusive evidence of their structure (that is, orientation of surfactant molecules at the gas–liquid interface, thickness of gas–liquid interface, and/or number of surfactant layers). Knowledge of the structure would enable us to use these dispersions more efficiently for their diverse applications (such as for removal of dyes, recovery of proteins, and enhancement of mass transfer in bioreactors). This study investigates dispersion and structural features of CGA utilizing a range of novel predictive (for prediction of aphron size and drainage rate) and experimental (electron microscopy and X-ray diffraction) methods. Results indicate structural differences between foams and CGA, which may have been caused by a multilayer structure of the latter as suggested by the electron and X-ray diffraction analysis.

Introduction

CGA (colloidal gas aphrons) are gas microbubbles (10–100 μm) created by stirring a surfactant solution at high speed (typically 8000 rpm). CGA have been characterized to some extent, for limited surfactants and under specific conditions (for review table see Jauregi et al., 1997) by several authors (Sebba, 1987; Save and Pangarkar, 1994; Jauregi et al., 1997; Chapalkar et al., 1993). It has been reported that these dispersions: (1) possess a large interfacial area; (2) exhibit relatively high stability; (3) separate easily from the bulk liquid phase; and (4) have similar flow properties to those of water. The identification of these properties has led researchers to consider CGA for various applications, such as removal of metals (Ciriello, 1982) and dyes (Roy et al., 1992), flotation of cells (Subramaniam et al., 1990; Hashim et al., 1998), protein recovery (Noble et al., 1998; Jauregi and Varley, 1998), and mass transfer in bioreactors (Bredwell and Worden, 1998).

Despite these characterization studies of CGA there is no conclusive evidence of the structure of these microbubbles. The structure of CGA was first proposed by Sebba (1987). Sebba claimed that CGA are not like conventional bubbles, which are surrounded by a surfactant monolayer, but are gas bubbles surrounded by three surfactant layers (see Figure 1). This theory was based on several experimental observations, including stability measurements. Sebba (1987) claimed that CGA can last for minutes or for hours, if stirring is maintained, without coalescence being appreciable. According to Sebba (1987), this is a result of the multilayer surfactant film surrounding the gas bubble, which delays coalescence. The evidence for the proposed CGA structure by Sebba (1987) is inconclusive. The current literature on CGA is mainly focused on the application of CGA, with the structure of CGA assumed to be that proposed by Sebba (1987).

Only two other studies have been reported in support of Sebba's proposed structure. First, Amiri and Woodburn (1990) presented a theoretical method to estimate the thickness of the surfactant "shell" in CGA. Amiri and Woodburn based their findings on a study of the liquid drainage rate in CGA dispersion and a calculation of aphron rise velocity.

Correspondence concerning this article should be addressed to J. Varley.

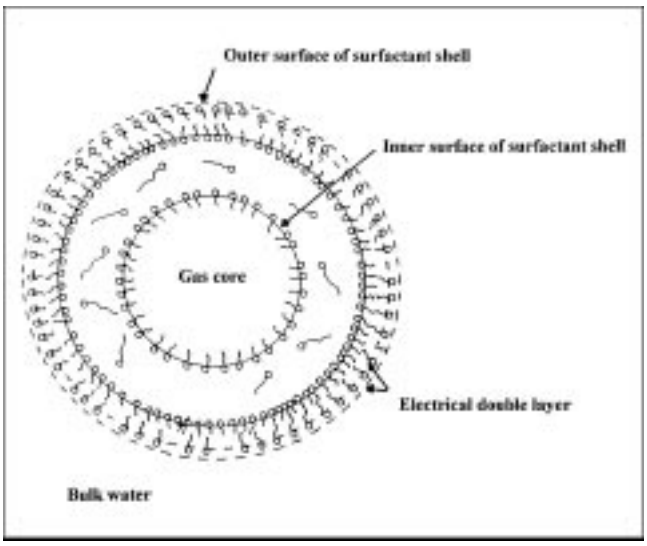

Figure 1. Structure of CGA proposed by Sebba (1987).

From these experimental results they concluded that CGA are composed of a finite interface of 750-nm thickness. This thickness is equivalent to 350 molecules of surfactant arranged in consecutive layers (if it is assumed that the length of a cetyltrimethyl ammonium bromide molecule, CTAB, is 2 nm). Second, Bredwell and Worden (1998) estimated the thickness of the surfactant (Tween 20) ''shell'' from a calculation of the mass-transfer coefficient in a fermenter using CGA in place of air bubbles (assuming that mass transfer is limited by the rate of diffusion across the shell). The estimated thickness ranged between 200 and 300 nm. Neither of these studies provides explicit evidence to validate Sebba's hypothesis, and it is also worth noting that the shell thicknesses estimated in the two studies differ significantly.

A knowledge of the structure of CGA would be very valuable for the optimization of CGA-based processes. For example, if the structure (such as number of surfactant layers and thickness of interface) were known, the mechanism of protein adsorption to CGA could be fully understood (Jauregi and Varley, 1998), and as a consequence optimization of CGA-based processes for protein recovery, including selective separation from mixtures, could be achieved.

In this article experimental measurements of the major dispersion and structural features of CGA are compared to predictions from models presented in the literature and in some cases, where appropriate, models have been modified. The major features considered are aphron diameter, stability (in terms of liquid drainage rate), and number of surfactant layers in the shell surrounding the gaseous core of each aphron (see Table 1).

In the literature, photographic techniques have been reported as the most commonly used techniques for measurement of bubble size in gas–liquid dispersions (Pinfold, 1972; Graham, 1976; Mita et al., 1978). Bee et al. (1986) reported the use of a light microscope combined with photographic and image-analysis techniques for measurement of bubble size in foams of high viscosity, stressing the difficulty of obtaining reliable measurements for dispersed gas phases. Ronteltap and Prins (1989) reported the use of an optical glass-fiber probe method to study the stability of foams by measuring bubble-size changes with time. In this study, measurements of aphron diameter made using microscopy together with image analysis techniques are presented. Theoretical models were also employed to predict aphron diameters. Prediction of aphron diameter has been carried out using two different models: (1) a model based on bubble breakup in agitated tanks (Parthasarathy et al., 1991), and (2) a model based on the prediction of liquid drainage rate of a CGA dispersion developed by Amiri and Woodburn (1990).

Stability is another important characteristic of CGA that will be influenced by their structure. Sebba (1987) stressed that due to his proposed structure (Figure 1) the coalescence of CGA is delayed, and hence these dispersions exhibit higher stability as compared to conventional foams. In the present work stability measurements for CGA are presented in terms of liquid drainage rates. A model that was developed for the prediction of liquid drainage rates of foams (Haas and Johnson, 1967) is applied for the prediction of liquid drainage rates of CGA dispersions. Also a modification to this model, proposed by Save and Pangarkar (1994), that accounts for possible structural differences of CGA is applied.

Finally two techniques of high resolving power—electron microscopy and X-ray diffraction—have been used in order to explore direct measurement of the structure of CGA. Several techniques have been developed for the study of high gas-phase dispersions that are inherently dynamic; these techniques involve freezing the sample (Wilson, 1996). In this way, the sample is fixed, that is, after freezing the liquid phase is immobilized, thus delaying any dynamic changes. Among these techniques freeze fracture for TEM (60 kV e-, $\lambda = 0.005$ nm) has the highest resolving power (maximum resolution of 0.3–0.5 nm). In the present study this technique has been used to determine the thickness of the CGA surfactant ''shell.''

The use of X-ray diffraction to determine the microstructure of gas–liquid dispersions is reported here for the first

Table 1. Predictive and Experimental Approaches Considered in This Study

Approach	Meas./Pred. Dispersion and Structural Features
Predictive model for bubble breakup in an agitated vessel (Parthasarathy et al., 1991)	Aphron diameter
Predictive model for liquid drainage rate in CGA (Amiri and Woodburn, 1990)	Aphron diameter
Predictive model for liquid drainage rate in a foam (Haas and Johnson, 1967)	Liquid drainage rate
Modified model of liquid drainage rate in a foam (Save and Pangarkar, 1994)	Liquid drainage rate
Electron microscopy	Thickness of the gas–liquid interface of aphrons
X-Ray diffraction	Number of surfactant layers and thickness of the interface

time. X-ray diffraction techniques have previously been used for the determination of microstructures in solution. For example, Kurumada et al. (1994) studied the formation of microstructures of oil-rich microemulsions composed of AOT (sodium bis-(2-ethyl hexyl) sulfosuccinate) and the phosphate derivative of this surfactant, sodium bis-(2-ethyl hexyl) phosphate using small-angle X-ray scattering (SAXS). Michel and Pileni (1994) determined by the same technique (SAXS) the structure of reverse micelles containing ribonuclease derivatives. In the present work, SAXS has also been used, but since gas–liquid dispersions (that is, CGA) contain little solid material (that is, more than 50% gas), a synchrotron source was used to provide an acceptable scattered signal.

From comparison of the experimental and predictive data for different types of gas–liquid dispersions, for example, foams and agitated tanks, it is expected to extract information regarding structural features of CGA.

Theory

Prediction of aphron diameter from prediction of liquid drainage rate of CGA

Once CGA have been generated (described in detail in the Experimental section) and when mixing of CGA ceases, CGA tend to rise due to the density difference between CGA and the bulk liquid phase. In addition, drainage of the liquid within the aphronic dispersion takes place. As a consequence, the aphron–liquid interface [$h_i(t)$] rises (see Figure 2iii). The interface rise velocity, $v(t)$, is proportional to the aphron rise velocity, $v_a(t)$, which in turn is a function of gas holdup and aphron diameter. These variables, that is, gas holdup and bubble diameter, change with time as drainage proceeds. Amiri and Woodburn (1990) considered that the aphron rise velocity just above the interface is equal to the observed rise velocity of the interface ($v_a(t) = v(t)$, assuming that no bubbles cross from below the interface). An expression for the rise velocity of the aphrons was developed by these authors as a function of gas holdup in the CGA dispersion and aphron diameter. In the present study Amiri and Woodburn's treatment is used for the prediction of aphron diameter. In addition, a different expression to that proposed by Amiri and Woodburn (1990) for the calculation of gas holdup in the CGA dispersion is proposed here. This expression is purely empirical and therefore does not rely on the assumptions needed for the definition proposed by Amiri and Woodburn (1990) (see below).

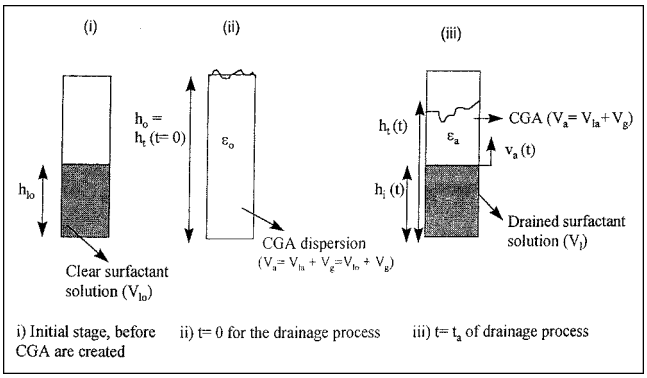

Figure 2. Drainage process for a CGA dispersion.

Diagram illustrates the different steps followed in the drainage study: (i) initial stage, clear surfactant solution before stirring begins (that is, no aphrons present); (ii) maximum dispersion volume just at point when stirring is stopped, start of drainage process (that is, $t = 0$); and (iii) as drainage progresses ($t = t_a$).

Gas Holdup in the Aphron Phase Above the Liquid Interface According to Amiri and Woodburn's Treatment (1990) (ϵ_a). By following Kynch's (1952) theory of sedimentation, $\epsilon_a(t)$ (Figure 2 iii) was calculated:

$$\epsilon_a(t) = \frac{h_o}{(h_o - h_a)} \times \epsilon_o, \tag{1}$$

where h_o is the height of the dispersion at $t = 0$ of drainage (Figure 2ii), and h_a is the coefficient of the drainage rate equation:

$$h_i(t) = h_a + v_a t, \tag{2}$$

where $h_i(t)$ is the interface (liquid–CGA) height.

Alternative Expression for Gas Holdup in the Aphron Phase Above the Liquid Interface (ϵ'). Gas holdup ϵ' is defined as the volumetric ratio of gas and dispersion:

$$\epsilon'(t) = V_g(t)/V_a(t), \tag{3}$$

where V_g and V_a are the volume of gas in the aphron phase and volume of aphron phase, respectively, and

$$V_g = V_a - V_{la} = V_a - (V_{lo} - V_l), \tag{4}$$

where V_{la} is the volume of liquid in the aphron phase, V_a is the volume of aphrons, V_{lo} is the initial (total) volume of liquid, and V_l is the volume of liquid drained from the aphron phase (Figure 2). Equation 4 can be rewritten in terms of height. Therefore, if h_t is the height at the top of dispersion, and h_{lo} is the initial height of liquid (Figure 2), using Eqs. 4 and 5, ϵ' is given by

$$\epsilon'(t) = \frac{V_a - V_{la}}{V_a} = \frac{V_a - (V_{lo} - V_l)}{V_a}$$

$$= \frac{(h_t - h_i) - (h_{lo} - h_i)}{(h_t - h_i)} = \frac{(h_t - h_{lo})}{(h_t - h_i)}. \tag{5}$$

At $t = 0$ of drainage $h_t = h_o$, $\epsilon' = \epsilon_o$, and therefore:

$$\epsilon' = \epsilon_o = \frac{(h_o - h_{lo})}{h_o}.$$

Calculation of the Aphron Rise Velocity. Amiri and Woodburn (1990) proposed that the aphron rise velocity, $v_a(t)$, can be calculated from a knowledge of the velocity of the bubbles rising in stagnant water, v_s, and the superficial velocity of the

displaced liquid flowing downward, v_{dw}. Thus:

$$v_a(t) = v_s - v_{dw} = v_s - \frac{\epsilon(t) \times v(t)}{[1-\epsilon(t)] \times \cos\theta},$$

where ϵ is the gas holdup in the aphronic phase (see Figure 2 iii), and it is assumed that the direction of the displaced flow is at an angle θ to the horizontal. With $v(t) = v_a(t)$ and considering $\cos\theta = 0.707$ (that is, $\theta = 45°$), the preceding equation can be rewritten as

$$v_a(t) = \frac{(1-\epsilon)}{(1-\epsilon+\epsilon/0.707)} \times v_s. \tag{6}$$

If it is assumed that the rise velocity of an aphron in stagnant water is given by Stoke's expression, the following equation can be derived for aphron diameter:

$$d = \sqrt{\frac{18 \times \mu_w}{(\rho_w - \rho_a) \times g} \times v_s}, \tag{7}$$

where d is the diameter of the aphrons, μ is the viscosity of the water, g is the gravity coefficient, ρ_w is the density of water, and ρ_a is the density of aphrons. The aphron velocity in stagnant water can be calculated from Eq. 6.

In addition to assumptions mentioned earlier, the following assumptions were made in this model:

- To calculate ϵ_a using Kynch's (1952) theory of sedimentation requires that the aphron should not coalesce or burst.
- Equations 6 and 7 for single aphrons are applied to a swarm of aphrons.
- The aphrons were assumed to be monosized and spherical.
- The variation of the aphron volume fraction, ϵ_a, with respect to height (z) was considered continuous with change in time.

Prediction of aphron diameter using equations derived for bubble breakup in gas–liquid dispersions in stirred tanks

As reported by Jauregi et al. (1997), power input used to create CGA is a critical factor for CGA formation. The level of energy input has an effect on the characteristics of CGA, including stability, gas holdup, and aphron diameter. Aphron diameter, gas holdup, and interfacial area are related since $A = 6\ \epsilon/d$ [if it is assumed that the aphrons are spherical (Tatterson, 1991)]. Bubble diameter has been correlated to power input (per unit of total dispersion volume) for bubble breakup in stirred vessels by a number of researchers (such as Tatterson, 1991; Calderbank, 1958). Several authors (such as Calderbank, 1958; Machon et al., 1997) have proposed correlations for maximum bubble diameter based on the concept of a critical Weber number (We_c) (where We is defined as inertial/surface tension forces). When We_c is exceeded, bubbles will break (Tatterson, 1991). Parthasarathy et al. (1991) suggested an equation, also based on a We_c for bubble break-up and Kolmogoroff's (1961) theory of local isotropic turbulence (see below). In addition Parthasarathy et al. (1991) considered: (1) the Sauter mean bubble diameter instead of the maximum bubble diameter with $d_{32}/d_{\max} = 0.62$ (Hesketh et al., 1987), and (2) the impeller swept volume (see below) instead of the total volume of the dispersion in the vessel. Conditions were noncoalescing (through surfactant addition). The expression proposed by Parthasarathy et al. (1991) for Sauter mean bubble diameter was

$$d_{32} = C_3 \left(\frac{\sigma^{3/5}}{(P/V_i)^{2/5} \rho^{1/5}} \right), \tag{8}$$

where ρ and σ are density and surface tension of the continuous phase, respectively, P is the power input, and V_i is the impeller swept volume ($\pi D^2 W/4$, where D and W are the diameter and width of the impeller, respectively) and C_3 is a proportionality constant related to We_c. In order to determine C_3, Parthasarathy et al. (1991) plotted the experimental values of d_{32} against the expression in brackets in Eq. 8. The proportionality constant C_3 was then estimated from the slope of the curve.

Assumptions made in this model

- Equation 8 is based on Kolmogoroff's (1961) local isotropic turbulence theory; the following conditions must be satisfied:
  1. Impeller Reynolds number ($Re = \rho N_i D^2/\mu) > 10^3$
  2. $L \gg d \gg \eta$,

where η is the length scale of energy dissipating eddies of the viscous subrange; L is the length scale for the primary eddies, which can be approximated to the length of the impeller blade width; and d is the bubble diameter. The length scale η is defined as follows:

$$\eta = (v^3/E)^{1/4}, \tag{9}$$

where v is the kinematic viscosity of the continuous phase, and E is the energy dissipation rate per unit mass. If the bubble size is larger than η, then the kinetic energy of the inertial subrange eddies is sufficient to break up the bubbles, and therefore the preceding equations will be applicable.

In the present study, a similar approach to that of Parthasarathy et al. (1991) has been followed to predict aphron diameters. This model was considered to be applicable because:

1. In CGA dispersion studies reported here, solution conditions were assumed to be noncoalescing.
2. CGA dispersions are generated at high speeds, that is, turbulent flow ($Re > 10^3$).
3. The range of aphron diameters was within the same range as that for bubble sizes measured by Parthasarathy et al. (1991).

Predictions of Liquid Drainage Rate for CGA Dispersions Using a Model for the Prediction of Liquid Drainage in a Foam

Haas and Johnson (1967) developed a model for the prediction of liquid drainage in a foam. In this model liquid

drainage in a foam was described as liquid flowing in capillaries of an equivalent diameter δ, that is, plateau borders. By applying a liquid-phase mass balance as a function of time, Haas and Johnson (1967) derived an expression for the liquid superficial velocity, L_o. From integration of the equation for liquid superficial velocity, between $t = t_o = 0$ (t_o being the disengagement time, that is, the time at which the foam–liquid interface starts rising at the bottom of the dispersion) and $t = t$, an expression for the accumulation of liquid drained, W, was obtained:

$$W(t, z_o) = L_o(t_o, z_o)\left[\frac{t - t_o}{cT_o(t - t_o) + 1}\right]. \qquad (10)$$

The constant cT_o can be evaluated from experimental values of $L_o(t_o, z_o)$ and $W(t_o, z_o)$. An expression for cT_o was derived as a function of $L_o(t_o, z_o)$:

$$cT_o = \left[\frac{\rho g}{32\mu}\frac{4}{\pi n k^2} \times \frac{4}{h_t^2} L_o(t_o, z_o)\right]^{1/2}. \qquad (11)$$

An abbreviated expression can be obtained for an aqueous foam, given the values for density and viscosity of water at 20°C are 998.20 kg/m^3 and 1.01×10^{-3} kg/ms, respectively; the number of plateau borders per unit cross-sectional area in a dry foam, $n = 2.5/d^2$; k is the ratio between the liquid holdup in the foam and the liquid holdup in the plateau borders and is taken as 1.5 (Haas and Johnson, 1967). The abbreviated expression is then,

$$cT_o = 526.10 \times \frac{dL_o^{1/2}}{h_t}, \qquad (12)$$

where $L_o(t_o, z_o)$ is the initial drainage rate, that is, $dh_i(t = t_o)/dt$, which is calculated from the initial linear part of the drainage rate slope (that is, dh_i/dt).

It has been shown in this study (see Results and Discussion and Tables 5 and 6), that aphron diameter varies during drainage. Therefore in order to calculate cT_o (Eq. 12) this variation in aphron diameter is taken into account with aphron diameter predicted at different times using Amiri and Woodburn's (1990) model (Eq. 7) [in Haas and Johnson's model (1967) bubble diameter was assumed constant].

The values given by Haas and Johnson (1967) for n and k are a result of geometrical and structural considerations of the foam. These authors considered that the foam was composed of dodecahedral bubbles. Save and Pangarkar (1994) investigated the drainage process in CGA and considered that CGA have different structural and dispersion features as compared to foams. As a result they modified the values of n and k in the following way:

- They assumed a higher content of liquid in CGA than in foams (that is, they assumed that a surfactant film surrounds the aphrons) and assumed that the proportionality constant $k = 2$.
- They modified the value of n, which assumes a dodecahedral structure of the foam, using an expression developed by Lemlich (1972), to determine the total length of capillaries per unit length of the vertical foam column:

$$N = \frac{7.81\, A_{\text{col}}\, \epsilon}{d^2},$$

where A_{col} is the cross-sectional area of the vessel, $n = N/A_{\text{col}}$, and ϵ is the gas holdup. This expression accounts for changes of the number of plateau borders with changes in gas holdup, that is, structural changes in the dispersion during the drainage process.

Using Save and Pangarkar's (1994) modification of Haas and Johnson's (1967) model, cT_o, denoted here as cT_o', is given by

$$cT_o' = 223.24 \times \frac{dL_o^{1/2}}{h_t \epsilon^{1/2}}. \qquad (13)$$

The corresponding interface height calculated using Eq. 13 in Eq. 10 is W' (with d' calculated from Eq. 7).

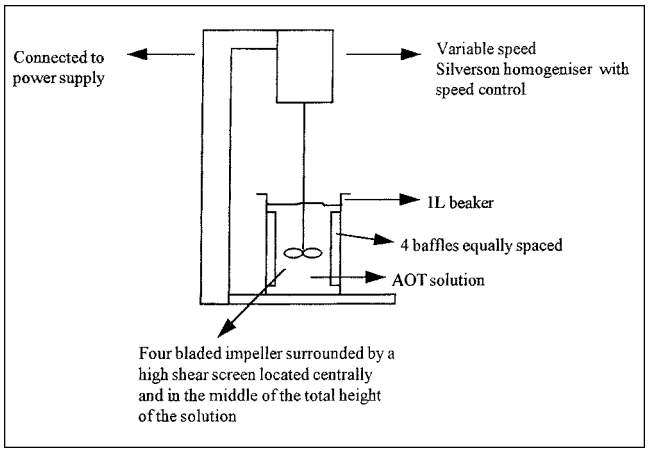

Figure 3. Stirring system used for the generation of CGA.

For more details, see Jauregi et al. (1997).

Experimental

Generation of CGA

A fully baffled beaker (volume = 1 L, diameter = 105 mm) containing a buffered solution (0.4 L) of AOT [sodium bis-(2-ethyl hexyl) sulfosuccinate] was stirred at speeds of 5000–10,000 rpm. Four baffles, equally spaced around the beaker each had dimensions of 120×10 mm. A laboratory mixer (SL2T model) fitted with a four-bladed impeller (D = 30 mm) surrounded by a high shear screen and with a digital readout for impeller speed, supplied by Silverson Ltd. (see Figure 3) was used. For each experiment, the stability of the aphrons (in terms of drainage rate, that is, dh_i/dt) and the gas holdup (ϵ' and ϵ_a) were measured.

Experimental measurement of aphron diameter

Size distributions for CGA samples from experiments carried out in a previous characterization study (Jauregi et al.,

Table 2. Statistical Design for the Characterization of CGA*

Exp.	C_s (mM)	pH	C_{st} (mM)	Time (min)	T (°C)	τ (s)	ϵ	T_f (°C)
1	0.1	4	0.00	4	1	90	0.17	29.0
2	0.1	4	0.00	16	2	107	0.32	20.0
3	0.1	4	0.14	4	2	45	0.17	22.0
4	0.1	4	0.14	16	1	30	0.12	43.0
5	0.1	8	0.00	4	2	90	0.26	23.0
6	0.1	8	0.00	16	1	68	0.32	41.0
7	0.1	8	0.14	4	1	60	0.20	27.0
8	0.1	8	0.14	16	2	75	0.28	20.0
9	61.0	4	0.00	4	2	420	0.50	23.0
10	61.0	4	0.00	16	1	840	0.57	35.5
11	61.0	4	0.14	4	1	290	0.44	25.5
12	61.0	4	0.14	16	2	306	0.46	19.0
13	61.0	8	0.00	4	1	594	0.53	25.4
14	61.0	8	0.00	16	2	710	0.57	18.0
15	61.0	8	0.14	4	2	180	0.40	21.0
16	61.0	8	0.14	16	1	163	0.50	34.0
17	0.1	6	0.07	10	1	60	0.27	36.0
18	61.0	6	0.07	10	1	249	0.52	30.0
19	0.1	6	0.07	10	2	80	0.23	24.0
20	61.0	6	0.07	10	2	220	0.51	24.0
21	2.5	4	0.07	10	1	160	0.49	32.0
22	2.5	8	0.07	10	1	152	0.51	32.0
23	2.5	4	0.07	10	2	170	0.50	19.0
24	2.5	8	0.07	10	2	120	0.49	21.0
25	2.5	6	0.00	10	1	372	0.61	32.0
26	2.5	6	0.14	10	1	115	0.36	36.0
27	2.5	6	0.00	10	2	375	0.59	23.4
28	2.5	6	0.14	10	2	90	0.30	21.0
29	2.5	6	0.07	4	1	150	0.36	27.0
30	2.5	6	0.07	16	1	140	0.53	38.0
31	2.5	6	0.07	4	2	110	0.25	24.0
32	2.5	6	0.07	16	2	150	0.51	25.0
33	2.5	6	0.07	10	1	128	0.47	34.0
34	2.5	6	0.07	10	1	140	0.46	34.0
35	2.5	6	0.07	10	1	145	0.49	33.0
36	2.5	6	0.07	10	2	133	0.48	24.0
37	2.5	6	0.07	10	2	140	0.46	19.0
38	2.5	6	0.07	10	2	150	0.47	25.0

*C_s, C_{st}, T, τ, and ϵ correspond to surfactant and salt concentration, temperature, stability, and gas holdup respectively (T_f is the temperature measured when stirring ceased).

1997; see Table 2 for experimental conditions) were determined using microscopy and image-analysis techniques. An Olympus light microscope connected to a CCD camera, model ICD-42E, Ikegami, from Tsushinki Co. Ltd., was used. The software used for the image analysis was pc_Image for windows supplied by Foster Findlay Associates Limited. The procedure was as follows:

1. A sample from the aphronic dispersion taken using a 5-μL syringe was placed on a microscope slide, magnified using a 4× magnification objective, and visualized on a computer screen.

2. During the first 2 min, after taking the sample from the beaker, different images from different areas of the sample were captured and stored for subsequent analysis.

3. Aphron size distributions, standard deviations, and coefficients of variability (% CV = s.d./mean × 100) were calculated for each data set.

Determination of Surfactant Concentration

Each sample was processed using the method described by Takagi et al. (1975) as follows:

1. Five mL of chloroform was added to a glass bottle. Then 1 mL of methylene blue, 0.007%, in aqueous solution of Na_2SO_4, 1%, was added, followed by 0.1 mL of sample.

2. The sample was vortexed for approximately 30 s.

3. The content of the bottle was poured into a test tube and the top layer (that is, the aqueous layer containing excess of the dye) was removed. The organic layer, which contained the surfactant–dye complex (surfactant and dye react one-to-one), was retained.

4. The extraction was repeated by washing the organic layer with 2 mL (approx.) of water.

5. The remaining water was removed (it would otherwise interfere with the readings) with Na_2SO_4.

6. The absorbance of the organic layer was measured at 650 nm.

7. A calibration curve for AOT concentration was prepared within the sensitivity range of the method (0.1–0.5 mM).

(The accuracy of this assay, as tested against overall mass balances, was within ±10%.)

Electron microscopy

The freeze fracture method used was jet freezing with propanol; this method was chosen as a result of the nature of the sample, that is, relatively stable with high content of gas. CGA were made by stirring the AOT solution (34 mM AOT in a 0.1-M acetate buffer at pH = 4) for 30 min. Sample replicas were mounted on copper grids before examination in an Hitachi H600 Transmission Electron Microscope operating at 75 kV. Photographs were taken of the replicas.

X-ray diffraction

In this work the small-angle scattering station (2.1) of Daresbury laboratory, Warrington, UK, was used. This station operates at a fixed wavelength using a crystal monochromator, $\lambda = 1.54$ Å, and at a variable camera length that provides spatial resolution ranging from 1 nm to 500 nm.

Solutions of AOT, prepared in a phosphate buffer (0.025 M, pH = 6), at different concentrations (below, at, and above the critical micelle concentration (cmc) of the surfactant) were used for the X-ray diffraction study. For each concentration, samples from two conditions were analyzed: (1) surfactant solution (with no CGA), and (2) CGA created from the same surfactant solution. Two different camera lengths (2 and 5 m) were used in each case. The surfactant solutions analyzed were: 0.6, 1.3, 2, 2.5, 30 and 61 mM.

A continuous flow cell (see Figure 4) was developed in order to study CGA samples for 3 h or more. CGA were created and pumped through the cell.

Scattering from each sample was recorded in terms of intensity of scattering (I) and channel numbers. In order to transform the raw data into graphs with meaningful scattering variables for the data analysis, a standard compound of a known scattering pattern, collagen from rat tail, was analyzed (calibration was carried out for each of the different camera lengths studied). This allowed the transformation of channel

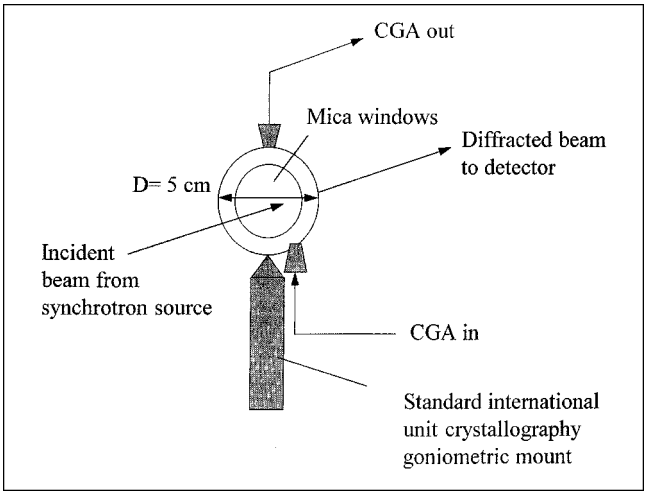

Figure 4. The continuous-flow cell developed for the X-ray diffraction study of CGA.

The small cylinder (diameter = 5 cm) with an adjustable sample length equipped with mica windows was designed for CGA to be pumped through continuously (the equipment was operated continuously for more than 3 h).

numbers into q values; q is the scattering vector and is $4\pi \sin\theta/\lambda$, where 2θ is the scattering angle and λ is the incident wavelength. Data were further transformed into Guinier plots, that is, $\ln(I)$ vs. q^2 (Guinier and Fournet, 1955). The slope of these plots was calculated, from which the radius of gyration (R_g) was determined. If a sphere of radius corresponding to the characteristic length, r, is taken as a model, from the radius of gyration and using some mathematical transformations (Stroud, 1987), a value for r, can be extracted. In this study the characteristic length corresponds to the thickness of the gas–liquid interface or the spacing between surfactant molecule layers.

Prediction of aphron diameter from liquid drainage of CGA using Amiri and Woodburn's (1990) model

The aphron diameters were determined using Stokes expression (Eq. 7). First the aphron rise velocity in stagnant water (v_s and v_s') was calculated from the corresponding gas holdup values (ϵ_a and ϵ', respectively) using Eq. 6. The gas holdups, ϵ_a and ϵ', were calculated from experimental data [$h_i(t)$ and $h_t(t)$] using Eqs. 1 and 5, respectively. The experimental value of v_a was calculated from the drainage curve, assuming that $v(t) = v_a = (dh_i/dt)$ (see earlier). From the equation of the slope (Eq. 2), h_a was calculated. Values for viscosity and density were taken as ρ_w (H_2O, 20°C) = 998.20 $kg \cdot m^{-3}$; ρ_a (aphrons) = 1.184 $kg \cdot m^{-3}$ (assuming ρ_a (aphrons) = ρ (air) at 20°C; that is, ignore surfactant shell); μ_w (H_2O, 20°C) = 1.01×10^{-3} $kg \cdot m^{-1} \cdot s^{-1}$.

Aphron diameters were calculated for eight experiments at different conditions of surfactant concentration (C_s), salt concentration (C_{st}), pH, and stirring time [it being known that these conditions have a large effect on stability (Jauregi et al., 1997)]. A summary of the experimental conditions is given in Table 3.

Prediction of aphron diameter using bubble breakup equations proposed by Parthasarathy et al. (1991)

In order to assess the applicability of Parthasarathy et al.'s model (1991) for conditions used in the study presented here, the length scale of the smaller eddies (Eq. 9) was calculated for the range of powers used (26–60 W). The range of values for η was 9–11 μm. These values are smaller than the measured aphron diameters (46–101 μm). It is therefore assumed that these aphrons can be broken up by the kinetic energy of the smaller eddies. The turbulence condition is also met (Reynolds $> 10^3$) and it was therefore decided that the model described earlier (Eq. 8) could be applied.

In order to predict aphron diameters using Eq. 8 the coefficient C_3 had to be estimated. The experimental Sauter mean bubble diameter values, $(d_{32})_e$, measured for each of the experiments in the characterization study (Table 2), were plotted against the expression in brackets in Eq. 8. The coefficient C_3 was then estimated from the slope of these curves.

Prediction of liquid drainage rate of CGA using a model for the prediction of drainage in a foam

In this study drainage curves were predicted following Haas and Johnson's (1967) and Save and Pangarkar's models (1994), but considering aphron diameter to be a function of time. Also Save and Pangarkar's model (1994) was applied directly, that is, the experimentally determined initial aphron diameter (assumed constant) was used for prediction of drainage rate. Drainage curves for experiments III, VII, and VIII (see Table 3) were determined using Eqs. 10–13. The resulting predicted drainage curves were compared to those obtained experimentally. The following steps were taken in order to calculate the predicted drainage curves:

- *Drainage rate calculated using Haas and Johnson's (1967) model, dW/dt, and a variable aphron diameter.* cT_o was calculated using the abbreviated expression in Eq. 12. The accumulated drained liquid, $W(t, z_o)$, which is equivalent to the parameter measured, $h_i(t)$, was calculated using Eq. 10. The disengagement time, t_o, was taken as zero and therefore $(t - t_o) = t$.

Table 3. Experimental and Predicted Aphron Diameters (for Initial Stage of Drainage, that is, Time Up to 2 min)*

Exp. No.	Experimental Conditions	Experimental		Predicted		
		d_{av} (μm)	d_{32} (μm)	d (7) (μm)	d' (7) (μm)	d_{32} (8) (μm)
I	61 mM/pH = 4/t = 4 min	46.3	59.9	9.2	n/a	77.1
II	0.56 mM/pH = 6/t = 10 min	n/a	n/a	28.9	n/a	67.0
III	0.1 mM/pH = 6/ 0.07 M NaCl/t = 10 min	57.9	75.5	36.9	51.1	66.3
IV	2.5 mM/pH = 8/ 0.07 M NaCl/t = 10 min	66.5	93.4	28.3	31.8	77.7
V	1.8 mM/pH = 6/t = 10 min	n/a	n/a	21.4	22.5	84.3
VI	0.71 mM/pH = 6/t = 10 min	45.7	57.1	26.9	28.2	69.4
VII	61 mM/pH = 8/t = 4 min	64.4	82.8	10.3	10.4	79.0
VIII	2.5 mM/pH = 6/t = 10 min	50.2	63.9	17.7	18.4	85.1

*The experimental conditions at which CGA were generated are surfactant conc./pH/salt conc./time of stirring. Equation numbers for predicted values are given in parentheses.

Table 4. Experimental and Predicted Aphron Diameters*

Exp.**	$P/V_i \times 10^{-6}$† (kW/m³)	$(d_{av})_e$ (μm)	$(d_{32})_e$ (μm)	$(d_{32})_p$ (μm)	Res‡ (%)
1	3.52	37.0	46.4	81.5	43.1
2	2.89	45.2	56.0	88.3	36.6
3	3.52	32.4	39.1	62.9	37.9
4	3.73	39.8	52.5	61.5	14.6
5	3.14	48.0	72.1	85.3	15.5
6	2.89	65.6	95.2	88.3	−7.8
7	3.39	50.5	85.9	63.9	−34.5
8	3.06	38.5	47.1	66.6	29.3
9	2.12	46.3	59.9	77.1	22.2
10	1.82	55.9	71.5	81.9	12.6
11	2.38	50.4	73.5	73.7	0.2
12	2.29	58.4	83.0	74.7	−11.1
13	1.99	64.4	82.8	79.0	−4.7
14	1.82	56.5	77.3	81.9	5.6
15	2.55	72.1	101.1	71.7	−41.1
16	2.12	62.7	93.0	77.1	−20.6
17	3.10	57.9	75.5	66.3	−14.0
18	2.04	58.8	86.9	78.3	−11.0
19	3.27	59.8	101.4	64.9	−56.3
20	2.08	64.1	98.0	77.7	−26.1
21	2.16	45.0	66.3	76.5	13.2
22	2.08	66.5	93.4	77.7	−20.2
23	2.12	49.4	82.1	77.1	−6.5
24	2.16	62.8	89.6	76.5	−17.1
25	1.65	50.2	63.9	85.1	25.0
26	2.72	49.1	85.8	69.8	−22.9
27	1.74	47.6	74.7	83.4	10.5
28	2.97	58.0	80.4	67.4	−19.3
29	2.72	59.6	81.5	69.8	−16.7
30	1.99	47.5	70.2	79.0	11.1
31	3.18	49.3	78.2	65.5	−19.4
32	2.08	48.8	87.4	77.7	−12.5
33	2.23	54.7	80.0	75.5	−5.9
36	2.25	44.2	63.2	75.3	16.1

*Predicted Sauter mean aphron diameter $(d_{32})_p$ was calculated using Eq. 8 with $C_3 = 1.5$. The volume swept by the impeller, V_i (m³), was calculated as 1.56×10^{-3} m³.
**See Table 2 for experimental conditions.
†Percentage residual, % Res = $[(d_{32})_p - (d_{32})_e]/(d_{32})_p \times 100$.
‡See Jauregi et al. (1997) for details of the calculation of power input.

• *Drainage rate calculated using Save and Pangarkar's (1994) model, dW′/dt, and a variable aphron diameter.* cT_o' was calculated using Eq. 13. The corresponding interface height calculated using Eq. 10 is W'.

• *Drainage rate calculated using Save and Pangarkar's (1994) model, dW″/dt.* cT_o'' was calculated by applying Save and Pangarkar's model in its unmodified form, that is, using an experimental average aphron diameter, $(d_{av})_e$, as d in the preceding equation. Using Eq. 13 and cT_o'', the corresponding interface height value, W'', was calculated (Eq. 10).

Results and Discussion

Experimental measurement of aphron diameter

Results of experimental measurements of aphron diameter in terms of average (that is, arithmetic mean) diameter, $(d_{av})_e$, and Sauter mean bubble diameter, $(d_{32})_e$ are shown in Table 4. Results for Sauter mean bubble diameter and average diameter show that diameters range between 39 and 101 μm and 32 and 72 μm, respectively, over the range of process parameters studied.

Table 5. Drainage Data and Aphron Diameter Measurement for Experiment VI (0.71 mM in Phosphate Buffer, 0.025 M, pH = 6, and Stirring Time = 10 min)*

t (s)	dh_i/dt (cm/s) $\times 10^{-2}$	ϵ_a (1)	ϵ' (5)	d (7) (μm)	d′ (7) (μm)	$(d_{av})_e$** (μm)
0	0.0	0.35	0.35	0.0	0.0	
18	1.1	0.35	0.36	19.0	19.1	
30	1.7	0.35	0.37	23.1	23.7	
39	3.3	0.33	0.38	32.1	34.0	
53	3.6	0.32	0.41	33.1	36.2	45.7
70	2.4	0.35	0.44	27.6	30.2	
84	3.6	0.31	0.47	32.9	38.7	
98	3.6	0.31	0.52	32.9	40.7	
117	3.2	0.33	0.58	31.4	41.6	
135	2.8	0.35	0.65	29.9	43.1	
161	1.2	0.48	0.70	22.1	30.2	54.0
225	0.5	0.59	0.74	16.2	20.6	
300	0.5	0.57	0.80	16.8	25.6	76.4
510	0.1	0.78	0.86	10.3	12.9	
613	0.1	0.78	0.90	10.3	15.7	

*The number in parentheses refers to the equation used to predict values given. Experimental average aphron diameters, $(d_{av})_e$, measured at different drainage times are also shown.
**Each $(d_{av})_e$ is effectively an average value over a 2-min period (see Experimental section). For comparison, predicted values should also be calculated as an average over this period.

Prediction of aphron diameter from liquid drainage of CGA using Amiri and Woodburn's (1990) model

Drainage data for experiments I–VIII were recorded. Only data for experiments VI and VII are presented here, as they are fully illustrative of the overall trends observed. Data (drainage rate, dh_i/dt, gas holdups, ϵ_a and ϵ', and corre-

Table 6. Drainage Data and Aphron Diameter Measurements for Experiment VII (61 mM AOT in Phosphate Buffer, 0.01 M, pH = 8, and Stirred for 4 min)*

t (s)	dh_i/dt (cm/s) $\times 10^{-2}$	ϵ_a (1)	ϵ' (5)	d (7) (μm)	d′ (7) (μm)	$(d_{av})_e$** (μm)
0	0.0	0.53	0.53	0.0	0.0	
90	0.2	0.53	0.54	10.3	10.4	64.4
155	0.5	0.52	0.55	14.7	15.3	
215	0.5	0.52	0.57	15.2	16.2	67.9
450	0.5	0.52	0.62	14.8	16.9	
580	0.5	0.51	0.67	15.6	19.6	71.9
690	0.5	0.53	0.71	14.7	19.3	
815	0.4	0.56	0.75	13.6	18.7	
1,065	0.3	0.61	0.81	12.4	18.4	115.6
1,325	0.2	0.69	0.86	10.9	16.8	
1,460	0.1	0.79	0.88	9.3	12.2	
1,740	0.1	0.79	0.90	9.2	13.2	
1,800	0.0	0.96	0.89	0.0	0.0	

*The number in parentheses refers to the equation used to predict values given. Experimental average aphron diameters, $(d_{av})_e$, measured at different drainage times are also shown.
**Each $(d_{av})_e$ is effectively an average value over a 2-min period (see Experimental section). For comparison, predicted values should also be calculated as an average over this period.

sponding values of aphron diameters, d and d', respectively) of experiments VI and VII are shown in Tables 5 and 6, respectively. These two experiments correspond to CGA of different stabilities, as illustrated by differences in their drainage rate profiles (dh_i/dt) (with CGA stability being greater for Experiment VI than for Experiment VII).

A larger variation in aphron diameter with time is predicted for dispersions with a lower stability and thus faster drainage rates and vice versa (Tables 5 and 6). The trend predicted by this model agrees with previous reports (such as Chapalkar et al., 1993), that is, that the higher the stability of the dispersion, the smaller the changes in the bubble diameter with time. Experimental results also support this observation (see Tables 5 and 6). In general, predictions from the model are closer to experimental observations for low concentrations, and predicted values are always significantly lower than experimental ones.

Gas holdup was determined using two different expressions: (1) ϵ_a (Eq. 1), and (ii) ϵ' (Eq. 5). From Tables 5 and 6, it can be seen that ϵ_a and ϵ' differ significantly at long drainage times; differences increase gradually as drainage progresses. Differences between the two values are larger for the lowest surfactant concentrations studied, generally before the drainage rate reaches a plateau (such as at 135 s in Table 5, and at 1,065 s in Table 6). This may be due to the assumption of noncoalescence in the calculation of ϵ_a (see above) (coalescence is likely to increase at longer drainage times). At longer drainage times, measurements of ϵ' are also subject to greater error, since the height of the aphron–air interface (h_t) is not so well defined at later stages of drainage. The values of ϵ' seem to vary more with time than do values of ϵ_a; also at a given time $\epsilon' > \epsilon_a$ (see Tables 5 and 6). The corresponding aphron diameters (d and d') do not differ significantly as drainage progresses; the main differences in aphron diameters are observed at the same time as maximum differences in gas holdups, that is, at long drainage times. Generally d' (aphron diameter based on ϵ') seem to be closer to the experimental values than d (aphron diameter based on ϵ_a). This reinforces the point made earlier that ϵ_a may be less accurate than ϵ'. At advanced stages of drainage, the model fails to predict aphron diameters, as indicated in Table 6 by a prediction of 0-μm aphron diameter when drainage reaches a plateau.

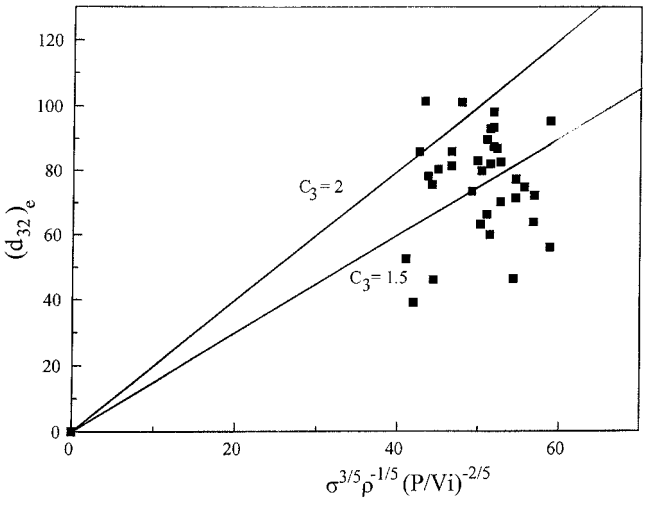

Figure 5. Prediction of Sauter mean bubble diameter from bubble break-up equations; plot for the estimation of C_3 (from Eq. 8).

Prediction of aphron diameter using bubble breakup equations proposed by Parthasarathy et al. (1991)

In order to estimate the coefficient C_3 (Eq. 8), the expression between brackets in Eq. 8 is plotted against experimental Sauter mean diameters $(d_{32})_e$ (see Figure 5). There is a lot of scatter in the data. The slope of the best-fit line (based on linear regression) was found to be 1.5 (see Figure 5) [a slope of 2 is also shown, as this was the value obtained by Parthasarathy et al. (1991)].

Predicted d_{32} values calculated using Eq. 8 and taking $C_3 = 1.5$ are shown in Table 4; experimental values are also given. Predicted values are all within a narrower range (60–90 μm) than experimental values (40–100 μm). The variation between each of the experimental and predicted values is given in Table 4 as % residual value (% Res) which is defined as

$$\% \text{ Res} = \frac{(d_{32})_p - (d_{32})_e}{(d_{32})_p} \times 100. \qquad (15)$$

The residual values in Table 4 vary between -56 and 43%. It is clear that not all the experimental variation in aphron diameters is predicted by Eq. 8. This could be due to the effect of, for example, surfactant and salt concentration on bubble diameter; these factors not being fully accounted for in Eq. 8. Surfactant and salt concentration will affect the surface-tension term of the equation; however, other effects, such as coalescence, are not accounted for. The model is based on the assumption that the effect of coalescence is insignificant (Machon et al., 1997). Coalescence will be important when surfactant concentration is low and when salt is added (since electrostatic repulsions will be suppressed).

Comparison of predictive models for aphron diameter

In Table 3 results of experimental and predicted aphron diameters measured in terms of average (d_{av}) and Sauter mean bubble diameter (d_{32}) are shown. These results correspond to the initial stages of drainage (time up to 2 min).

The variation of aphron diameter with surfactant concentration follows a different trend dependent on the method used for predicting aphron diameter. The model based on drainage rate predicts a decrease of aphron diameter as surfactant concentration increases (see results of experiments II, V, VI, and VIII in Table 3). The higher the surfactant concentration, the higher the stability of the dispersion and the lower the drainage rate. Thus, according to this model, high stability dispersions contain smaller aphrons. However, the opposite trend is predicted by the model based on bubble breakup, that is, aphron diameters increase with increasing surfactant concentration. In the bubble breakup model, bubble (aphron) diameters are described as a function of surface tension and power input. The model predicts a reduction in bubble (aphron) diameter as surface tension decreases. Sur-

face tension will decrease as surfactant concentration increases up to the critical micelle concentration (cmc) of the surfactant. In this study, surfactant concentration is for most conditions above or close to the cmc, thus the surface-tension term does not change significantly. Therefore, aphron diameter will mainly change due to the variation in power input, which varies with the gas holdup (Jauregi et al., 1997). The bubble breakup model predicts a reduction in bubble diameter as power input increases. In this work CGA are created at a constant speed with the power input increasing with decreasing gas holdup (that is, with a decrease in surfactant concentration). Experimentally measured average and Sauter mean aphron diameters follow the same trend (see experiments VI–VIII in Table 3) as that predicted by the bubble breakup model.

Overall the aphron diameters predicted by the bubble breakup model are closer to the experimental values than those predicted by the model based on liquid drainage through a ''static'' gas–liquid dispersion. However, from the preceding results it can be concluded that the bubble breakup model does not fully predict the breakup of aphrons in CGA dispersions.

Prediction of liquid drainage rate of CGA using a model for the prediction of drainage in a foam

Results for liquid drainage rates corresponding to experiments VII and III are shown in Figures 6 and 7. Four drainage curves are plotted in each graph: (1) dh_i/dt, the experimental drainage curve; (2) dW/dt, with cT_o (Eq. 12); (3) dW'/dt, with cT_o' (Eq. 13); (iv) dW''/dt, with cT_o'' [Eq. 13 and $(d_{av})_e$ = constant].

Results in Figure 6 (Experiment VII) indicate that the prediction of the model improves when a variable aphron diameter is considered, as proposed in the present study, and also when Save and Pangarkar's modification is applied, that is, dW'/dt is closer to experimental data than dW/dt. Save and Pangarkar's model prediction (dW'/dt) is worse in the later stages of drainage (the last two points in Figure 6). Experiment VIII showed similar trends.

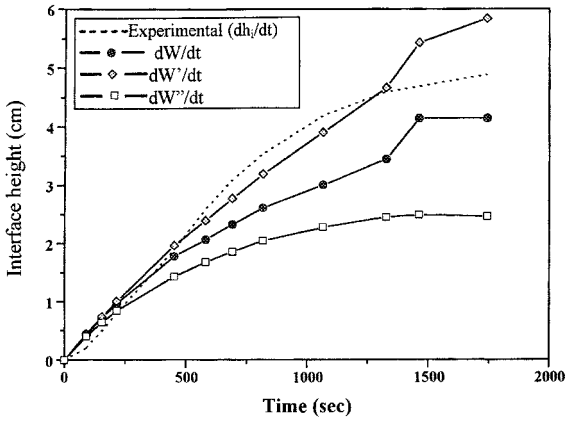

Figure 6. Prediction of drainage rate for experiment VII (61 mM AOT in phosphate buffer 0.01 M, pH = 8, and stirred for 4 min) using the foam drainage model (Eqs. 12 and 13).

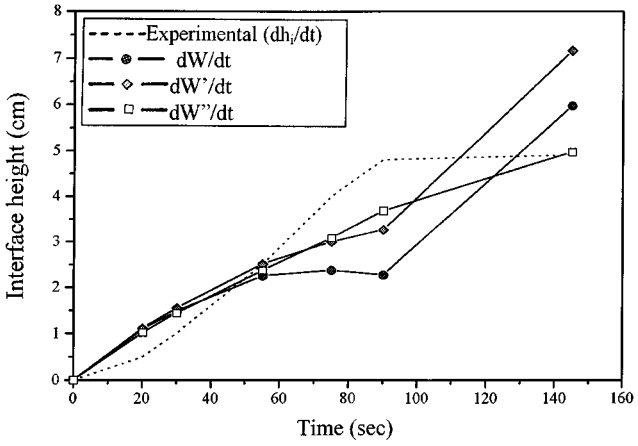

Figure 7. Prediction of drainage rate for experiment III (0.1 mM AOT in phosphate buffer, 0.025 M, pH = 6 and stirred for 10 min) using the foam drainage model (Eqs. 12 and 13).

In Figure 7 drainage curves corresponding to Experiment III are shown. The two drainage curves corresponding to the model with Save and Pangarkar's modification, dW'/dt and dW''/dt are the closest to the experimental curve. These two curves differ very little, but when drainage reaches a plateau the curve corresponding to the model in which the experimental aphron diameters are assumed constant, dW''/dt, gives a closer prediction of drainage than when a variable bubble size is considered, dW'/dt.

From the three cases studied, it can be concluded that the drainage curve corresponding to the foam model with Save and Pangarkar's modification, which takes into account structural features of CGA (that is, liquid film surrounding the aphrons and nondodecahedral structure), further modified here to account for the variation of aphron diameter with time, gives the best fit to the experimental data (that is, dW'/dt best fits the experimental data). This demonstrates that there are structural differences between conventional foams and CGA. (Toward the end of drainage the prediction of this model gets worse; the most probable explanation being that this model depends on prediction of aphron diameter from Amiri and Woodburn's model, which earlier was shown to fail to predict aphron diameter at advanced stages of drainage.)

Study of the structure of CGA using electron microscopy

One of the images captured using electron microscopy is shown in Figure 8 (the magnification is 250,000, or 1 mm = 4 nm). The light area corresponds to the gas (air) phase and the dark area corresponds to the liquid phase of the dispersion. The gas–liquid interface is defined by two lines of similar thickness and dark color. The total interfacial area has an average thickness of 96 nm. The length of an AOT molecule tail (hydrophobic part) is around 8.3 Å and the diameter of the polar head is around 3.5 Å (Gupta et al., 1994), so the total length of an AOT molecule is 12 Å or 1.2 nm, and therefore around 80 molecules of surfactant could fit in this interface (this does not allow for an inner water phase of

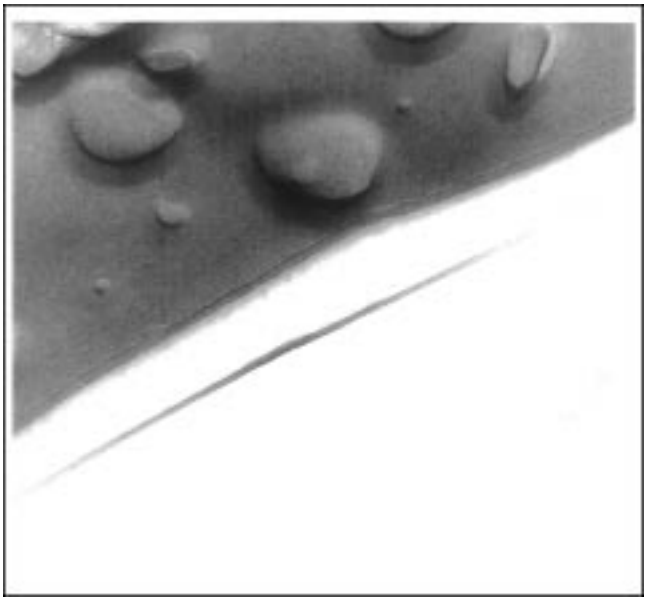

Figure 8. Electron micrograph of CGA (34 mM AOT in an acetate buffer, 0.1 M and pH = 4).

A transmission electron microscope (TEM) was used; the sample being prepared using the freeze fracture method.

finite thickness, as included in Sebba's original proposed structure of CGA; see Figure 1). This estimated thickness is lower than that estimated by Amiri and Woodburn (1990), that is, 750 nm, for a cationic surfactant, CTAB (2 nm long approximately) and Bredwell and Worden (1998), that is, 200–300 nm for a nonionic surfactant, Tween 20 (the approximate length of the fatty acid fraction, that is, hydrophobic tail, will be in a range between 2 and 7 nm).

Study of the structure of CGA using small angle X-ray diffraction

The calculation of the characteristic length from the scattering data is subject to several approximations:

- The calculation of the slope from the Guinier plot may be subject to error, since in some cases different slopes could be fitted to the curves. This is particularly true for the plots corresponding to long camera lengths. A possible reason could be that there is a distribution of sizes corresponding to different structures of aphrons with a variable number of surfactant layers.
- In order to calculate the characteristic length, a model must be assumed. In this study a solid sphere was taken as a model and then the characteristic length was calculated from the radius of gyration data.

Preliminary results obtained at a long camera length are shown in Table 7. It is interesting to note that the scattering of a sample of a surfactant concentration without aphrons is significantly different to that of a sample of the same surfactant concentration but with aphrons, as indicated by the R_g values calculated from the slope of the scattering curve (see Table 7).

In Table 7 the number of surfactant molecules (n_s) corresponding to the characteristic length (r) calculated from the

Table 7. Results from the X-Ray Diffraction Analysis of AOT Solutions of Variable Concentration and Their Corresponding CGA (Camera Length = 5 m)*

Sample	C_s (mM)	R_g (Å)	r (Å)	n_s
Aphrons	0.6**	62	98.0	8.2
	1.3	55	87.0	7.2
	2	61	96.4	8.0
	2.5**	53	83.8	7.0
	30**	59	93.3	7.8
	61**	52	82.2	6.9
	Avg.	**57**	**90.1**	**7.5**
No aphrons	0.6**	14	22.1	1.8
	1.3	13	20.6	1.7
	2	13	20.6	1.7
	2.5**	23	36.4	3.0
	30**	39	61.7	5.1
	61**	39	61.7	5.1

*The radius of gyration, R_g, and the corresponding characteristic length, r, are shown. The number of surfactant molecules equivalent to the characteristic length, n_s, is also calculated assuming the length of an AOT molecule is 12 Å.

**Scattering of these solutions was also studied at a short camera length.

Guinier plots is shown. This is determined assuming that the length of an AOT molecule is 1.2 nm (Gupta et al., 1994). The number of surfactant molecules corresponding to the characteristic length is 2 for samples containing solutions (no aphrons) of 0.6, 1.3, and 2 mM AOT (see Table 7). Thus the scattering signal is probably due to micelles of diameter corresponding to the length of two surfactant molecules. At higher surfactant concentrations, for example, 2.5, 30, and 61 mM, an increase in radius of gyration is observed with a subsequent increase in the characteristic length. At these concentrations of AOT, surfactant molecules form lamellar structures (Alexopoulos et al., 1989). Therefore the scattering signal could correspond to 3–5 molecules of surfactant arranged in subsequent sheets/layers.

Samples containing aphrons give similar scattering regardless of the surfactant concentration, as indicated by the calculated radius of gyration; using the short and long camera length, the average (averaged over the different surfactant concentrations studied) radius of gyration was 54 (s.d. = 3.6) Å and 57 (s.d. = 4.2) Å, respectively. The number of surfactant molecules corresponding to these radii of gyration are 7 and 7.5, respectively (see Table 7). Thus the scattering results indicate that the shell surrounding the aphrons is composed of more than one layer of surfactant (the exact number of layers cannot be determined due to the approximations mentioned before) and that the same structure of aphrons is obtained when working at different surfactant concentrations.

Other supporting evidence for the existence of multilayers of surfactant surrounding gas bubbles in CGA dispersions

In a previous report by the authors (Jauregi et al., 1997), stability studies were carried out at variable stirring speeds (power input). Jauregi et al. (1997) found that there was a critical speed above which stability and gas holdup increase dramatically at any surfactant concentration (below, about, and above the surfactant cmc) and also that a minimum energy is necessary in order to generate CGA of measurable

stability. These results suggest that the formation of CGA dispersions goes through a transition after which a more stable dispersion is obtained. During this transition arrangement of surfactant molecules in multilayers may occur as proposed by Sebba (1987).

Conclusions

Aphron diameters have been predicted using models previously proposed for bubble breakup in agitated vessels and for liquid drainage in foam and CGA dispersions. Although the aphron diameters predicted by the bubble breakup model are closer to the experimental values than those predicted by the model based on liquid drainage for CGA dispersions, neither model satisfactorily predicts aphron diameters. Of the models considered for prediction of liquid drainage in CGA dispersions, that proposed by Save and Pangarkar (1994), which is based on assumptions including the existence of a liquid film surrounding the aphrons and a nondodecahedral structure (a dodecahedral structure often being assumed for conventional foams) further modified here to account for the variation in aphron diameter with time, gives the best fit to the experimental data. The experimental and model results presented here support the hypothesis that CGA dispersions have different structural and dispersion features than either conventional foams or noncoalescing gas–liquid dispersions (with relatively low gas holdups) formed in agitated vessels. These differences could be due to the existence of multilayers of surfactant orientated around the gas bubbles, as proposed by Sebba. In an attempt to gain further information on the structure of CGA (that is, thickness of interface and number of layers), two high resolving power techniques–electron microscopy and X-ray diffraction—were applied to CGA dispersions. Although the use of these techniques for CGA needs to be developed further, preliminary results indicate the existence of an interface composed of more than one layer. Furthermore, in this study the use of X-ray diffraction has been presented for the first time to investigate the structure of gas–liquid dispersions such as CGA, and its potential has been proved.

Acknowledgments

The authors thank the Basque Government and the BBSRC for their financial support. They also extend their gratitude to the Microscopy group in the Institute of Food Research, Reading laboratory for their collaboration in the microscopy work, the SRS at Daresbury laboratory for allowing them to use their facilities, and Mathew Noble from their research group for his collaboration in the analysis of the X-ray diffraction data.

Notation

A = interfacial area, m^2/m^3
cT_o' = time for the prediction of drainage rate obtained using Save and Pangarkar's modification to the model, s^{-1}
cT_o'' = time for the prediction of drainage rate obtained using Save and Pangarkar's modification to the model and the experimental bubble size, s^{-1}
d_{max} = maximum bubble diameter reached before breakup by turbulence, m
Ni = rotational speed, s^{-1}
W' = predicted accumulated drained liquid calculated from cT_o', cm
W'' = predicted accumulated drained liquid calculated from cT_o'', cm
z_o = foam/liquid interface height, m

Literature Cited

Alexopoulos, A. H., J. E. Puig, and E. I. Franses, "Phase Continuity and Surface Properties of Dispersions of AOT/Water Liquid Crystals," *J. Colloid Interface Sci*., **128**, 27 (1989).
Amiri, M. C., and E. T. Woodburn, "A Method for the Characterisation of Colloidal Gas Aphrons Dispersions," *Trans. Inst. Chem. Eng*., **68**, 154 (1990).
Bee, R. D., A. Clements, and A. Prins, "Behavior of an Aerated Food Model," *Food Colloids*, Vol. 58, E. Dickinson, ed., Royal Society of Chemistry, Special Publications, Royal Society of Chemistry, Cambridge, p. 128 (1986).
Bredwell, M. D., and R. M. Worden, "Mass-Transfer Properties of Microbubbles: 1. Experimental Studies," *Biotechnol. Progr*., **14**, 31 (1998).
Calderbank, P. H., "Physical Rate Processes in Industrial Fermentation. Part I: The Interfacial Area in Gas-Liquid Contacting with Mechanical Agitation," *Trans. Inst. Chem. Eng*., **36**, 443 (1958).
Chapalkar, P. G., K. T. Valsaraj, and D. Roy, "A Study of the Size Distribution and Stability of Colloidal Gas Aphrons Using a Particle Analyzer," *Sep. Sci. Technol*., **28**, 1287 (1993).
Ciriello, S., S. M. Barnett, and F. J. Deluise, "Removal of Heavy Metals from Aqueous Solutions Using Microgas Dispersions," *Sep. Sci. Technol*., **17**, 521 (1982).
Graham, D. E., "Structures of Adsorbed Protein Films and Stability of Foams and Emulsions," PhD Thesis, London University (1976).
Guinier, A., and G. Fournet, *Small Angle Scattering of X-Rays*, Wiley, New York (1955).
Gupta, R. B., C. J. Han, and K. P. Johnston, "Recovery of Proteins and Amino Acids from Reverse Micelles by Dehydration with Molecular Sieves," *Biotechnol. Bioeng*., **44**, 830 (1994).
Haas, P. A., and H. F. Johnson, "A Model and Experimental Results for Drainage of Solution Between Foam Bubbles," *Ind. Eng. Chem. Fundam*., **6**, 225 (1967).
Hashim, M. A., B. Sengupta, S. V. Kumar, R. Lim, S. E. Lim, and C. C. Tan, "Effect of Air to Solid Ratio in the Clarification of Yeast by Colloidal Gas Aphrons," *J. Chem. Technol. Biotechnol*., **71**, 335 (1998).
Hesketh, R. P., T. W. Fraser Russel, and A. W. Etchells, "Bubble Size in Horizontal Pipelines," *AIChE J*., **33**, 663 (1987).
Jauregi, P., S. Gilmour, and J. Varley, "Characterisation of Colloidal Gas Aphrons for Subsequent Use for Protein Recovery," *Chem. Eng. J*., **65**, 1 (1997).
Jauregi, P., and J. Varley, "Colloidal Gas Aphrons (CGA): A Novel Approach to Protein Recovery," *Biotechnol. Bioeng*., **59**(4), 471 (1998).
Kolmogoroff, A. N., "Dissipation of Energy in the Locally Isotropic Turbulence," *Turbulence. Classic Papers on Statistical Theory*, S. K. Friedlander and L. Topper, eds., Interscience, New York (1961).
Kurumada, K., A. Shioi, and M. Harada, "Microstructures of Concentrated Water-in-Oil Microemulsions in Sodium Bis(2-ethylhexyl) Sulfosuccinate and Sodium Bis(2-ethylhexyl) Phosphate Systems," *J. Phys. Chem*., **98**, 12382 (1994).
Kynch, G. J., "A Theory of Sedimentation," *Trans. Faraday Soc*., **48**, 166 (1952).
Lemlich, R., "Principles of Foam Fractionation and Drainage," *Adsorptive Bubble Separation Techniques*, Chap. 3, R. Lemlich, ed., Academic Press, New York, p. 33 (1972).
Machon, V., A. W. Pacek, and A. W. Nienow, "Bubble Sizes in Electrolyte and Alcohol Solutions in a Turbulent Stirred Vessel," *Trans. Inst. Chem. Eng*., **75**(A), 339 (1997).
Michel, F., and M. P. Pileni, "Synthesis of Hydrophobic Ribonuclease by Using Reverse Micelles. Structural Study of AOT Reverse Micelles Containing Ribonuclease Derivatives," *Langmuir*, **10**, 390 (1994).
Mita, T., E. Ishida, and H. Matsumoto, "Physicochemical Studies on Wheat Protein Foams: II. Relationship Between Bubble Size and Stability of Foams Prepared with Gluten Components," *J. Colloid Interface Sci*., **64**(1), 143 (1978).
Noble, M., A. Brown, P. Jauregi, A. Kaul, and J. Varley, "Protein

Recovery Using Gas-Liquid Dispersions,'' *J. Chromatogr. B*, **711**, 31 (1998).
Parthasarathy, R., G. J. Jameson, and N. Ahmed, ''Bubble Break-up in Stirred Vessels. Predicting the Sauter Mean Diameter,'' *Trans. Inst. Chem. Eng*., **69**, 295 (1991).
Pinfold, T. A., ''Ion Flotation,'' *Adsorptive Bubble Separation Techniques*, Chap. 4, R. Lemlich, ed., Academic Press, New York, p. 53 (1972).
Ronteltap, A. D., and A. Prins, ''Contribution of Drainage, Coalescence, and Disproportionation to the Stability of Aerated Foodstuffs and the Consequences for the Bubble Size Distribution as Measured by a Newly Developed Optical Glass-Fibre Technique,'' *Food Colloids*, Vol. 75, R. D. Bee, P. Richmond, and J. Mingins, eds., The Royal Society of Chemistry Special Publications, Roy. Soc. of Chemistry, Cambridge, p. 39 (1989).
Roy, D., K. T. Valsaraj, and S. A. Kottai, ''Separation of Organic Dyes from Wastewater by Using Colloidal Gas Aphrons,'' *Sep. Sci. Technol*., **25**, 573 (1992).
Save, S. V., and V. G. Pangarkar, ''Characterisation of Colloidal Gas Aphrons,'' *Chem. Eng. Commun*., **127**, 35 (1994).
Sebba, F., *Foams and Biliquid Foams-Aphrons*, Wiley, Chichester, England (1987).
Stroud, K. A., *Engineering Mathematics*, 3rd ed., Macmillan, London (1987).
Subramaniam, M. B., N. Blakebrough, and M. A. Hashim, ''Clarification of Suspensions by Colloidal Gas Aphrons,'' *J. Chem. Technol. Biotechnol*., **48**, 41 (1990).
Takagi, T., K. Tsujil, and K. Shirahama, ''Binding Isotherms of Sodium Dodecyl Sulfate to Protein Polypeptides with Special Reference to SDS-Polyacrilamide Gel Electrophoresis,'' *J. Biochem*., **77**, 939 (1975).
Tatterson, G. B., ''Gas Dispersion in Agitated Tanks,'' *Fluid Mixing and Gas Dispersion in Agitated Tanks*, McGraw-Hill, London (1991).
Wilson, A., ''Experimental Techniques for the Characterisation of Foams,'' *Foams: Theory, Measurements and Applications*, R. K. Prud'homme and S. A. Khan, eds., Dekker, New York (1996).

Manuscript received Jan. 25, 1999, and revision received Aug. 9, 1999.